Low Energy Collisions

V.I. Baranov

Binary collision in the laboratory frame of reference (planar)

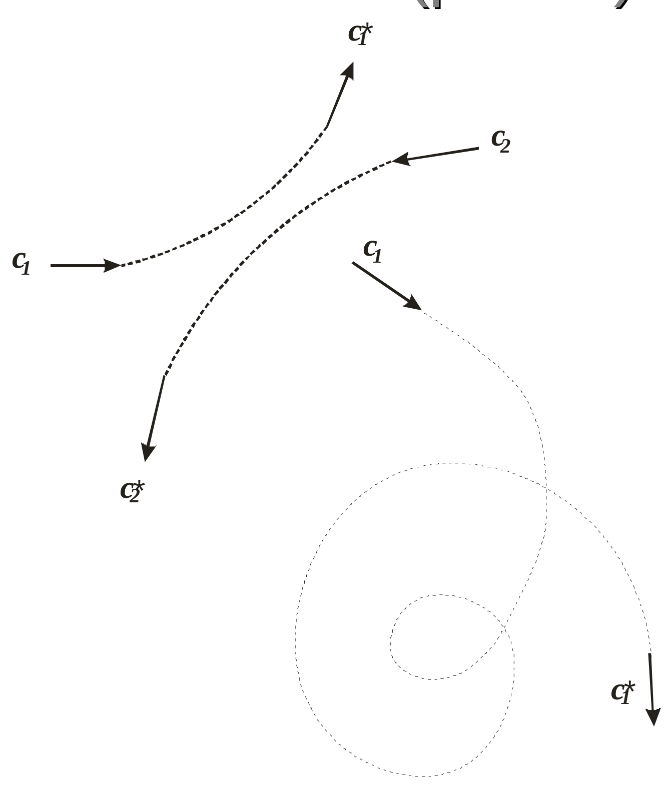

Binary elastic collisions

$$m_1\mathbf{c_1} + m_2\mathbf{c_2} = m_1\mathbf{c}_1^* + m_2\mathbf{c}_2^* = (m_1 + m_2)\mathbf{c_m}$$

$$m_1 c_1^2 + m_2 c_2^2 = m_1 c_1^{*2} + m_2 c_2^{*2}$$

Conservation of momentum & energy

$$\mathbf{c_r} = \mathbf{c_1} - \mathbf{c_2}$$

Relative velocity

$$m_r = \frac{m_1 m_2}{m_1 + m_2}$$

Reduced mass

Binary collision in the centre of mass frame of reference

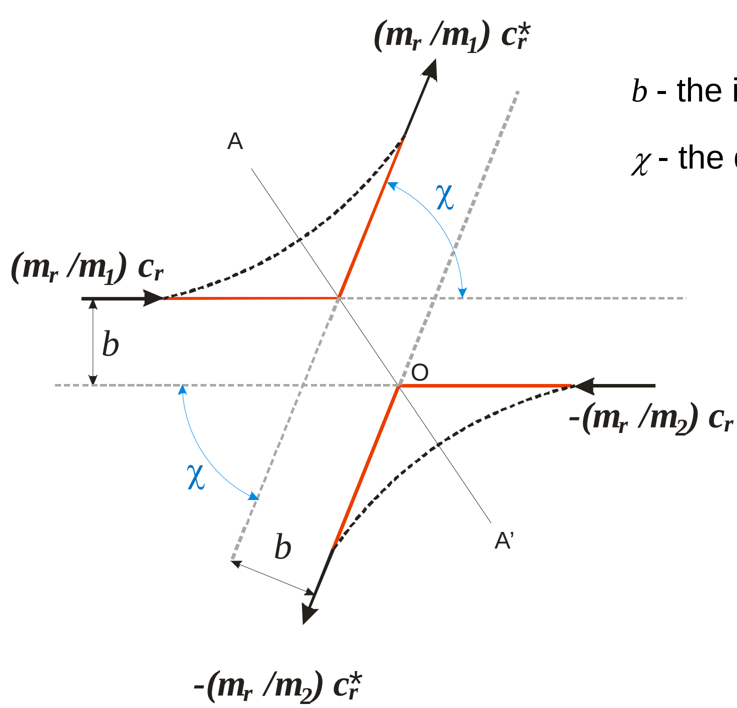

b - the impact parameter

χ - the deflection angle

Collision of the reduced mass particle with a fixed scattering centre

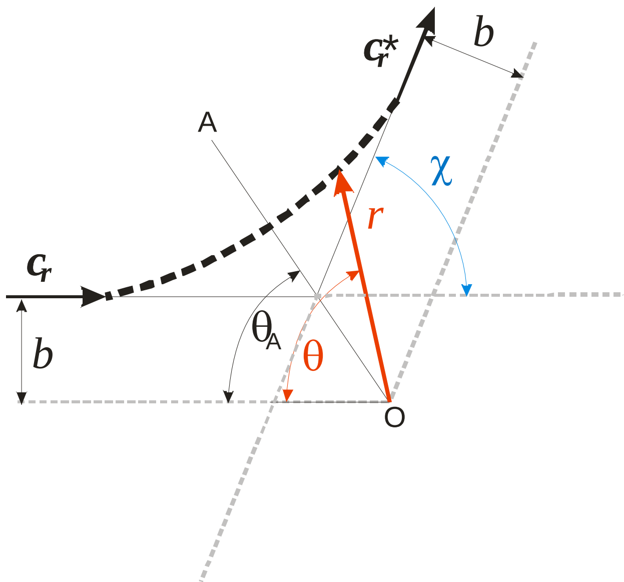

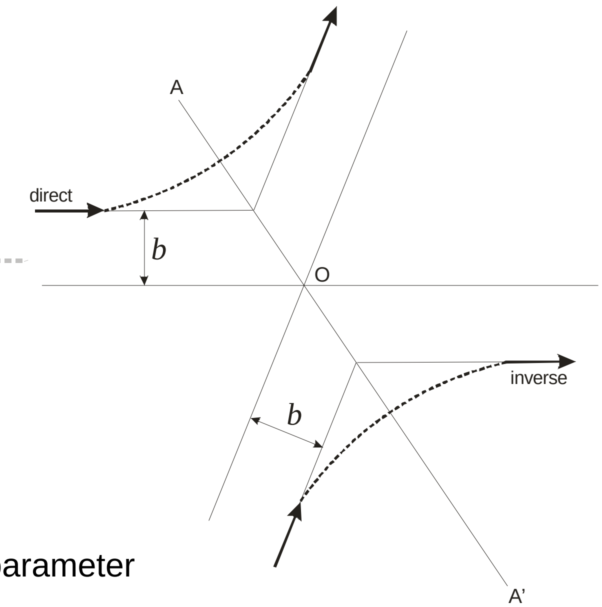

b - the impact parameter

χ - the deflection angle

Collision cross-section

b - the impact parameter

χ - the deflection angle

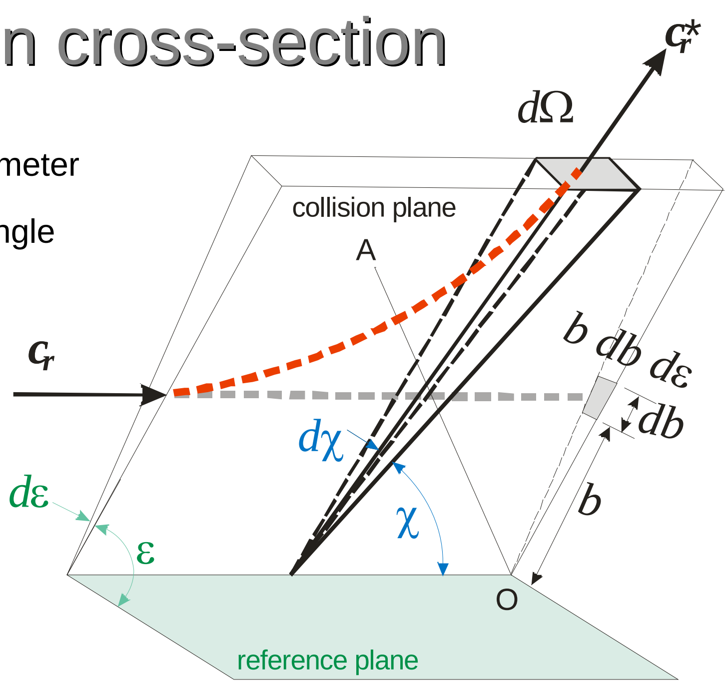

$$\left.\begin{aligned} \sigma\, d\Omega &= b\, db\, d\varepsilon \\ d\Omega &= \sin\chi\, d\chi\, d\varepsilon \end{aligned}\right\} \rightarrow \sigma = \frac{b}{\sin\chi}\left|\frac{db}{d\chi}\right|; \quad \sigma_T = \int_0^{4\pi} \sigma\, d\Omega = 2\pi \int_0^{2\pi} \sigma \sin\chi\, d\chi$$

Collision cross-sections

The total cross-section

$$\sigma_T = \int_0^{4\pi} \sigma \, d\Omega = 2\pi \int_0^{2\pi} \sigma \sin\chi \, d\chi$$

The viscosity cross-section

$$\sigma_\mu = \int_0^{4\pi} \sigma \sin^2\chi \, d\Omega = 2\pi \int_0^{\pi} \sigma \sin^3\chi \, d\chi$$

The momentum transfer (diffusion) cross-section

$$\sigma_M = \int_0^{4\pi} \sigma \left(1-\cos\chi\right) d\Omega = 2\pi \int_0^{\pi} \sigma \left(1-\cos\chi\right) \sin\chi \, d\chi$$

The hard sphere model

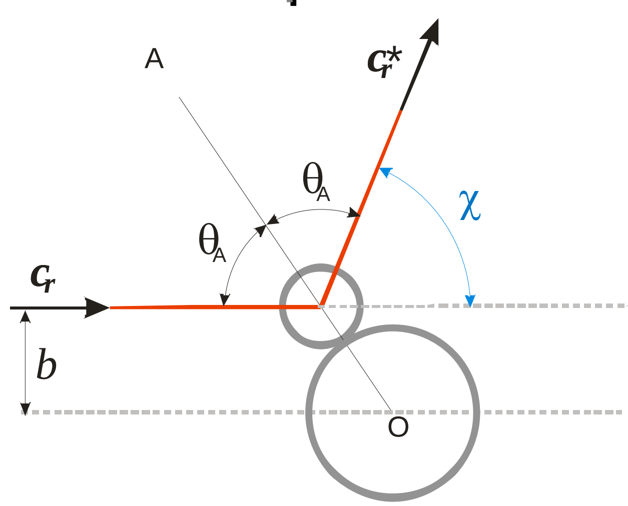

$$\left.\begin{aligned} d_{12} &= \tfrac{1}{2}\left(d_1 + d_2\right) \\ b &= d_{12}\sin\theta_A = d_{12}\cos\left(\tfrac{1}{2}\chi\right) \end{aligned}\right\} \rightarrow \left|\frac{db}{d\chi}\right| = \tfrac{1}{2} d_{12}\sin\left(\tfrac{1}{2}\chi\right) \rightarrow \sigma = \tfrac{1}{4} d_{12}^2$$

$$\sigma_T = 2\pi \int_0^{2\pi} \sigma \sin\chi \, d\chi = \pi d_{12}^2$$

Hard sphere collision cross-sections

The total cross-section

$$\sigma_T = \pi d_{12}^2$$

The viscosity cross-section

$$\sigma_\mu = \tfrac{2}{3}\sigma_T$$

The momentum transfer (diffusion) cross-section

$$\sigma_M = \sigma_T$$

The summation invariants (conservation of mass, momentum and energy)

$$C$$

$$\mathbf{B}\bullet m\mathbf{c}$$ scalar product

$$A\tfrac{1}{2}mc^2$$

$$A\tfrac{1}{2}mc^2 + \mathbf{B}\bullet m\mathbf{c} + C$$

Equilibrium state. Maxwellian distribution function

Isotropic distribution

$$\left.\begin{aligned} f_1^* f_2^* - f_1 f_2 &= 0 \\ \ln f_1^* + \ln f_2^* &= \ln f_1 + \ln f_2 \end{aligned}\right\} \rightarrow \ln f = A \tfrac{1}{2} mc^2 + \mathbf{B} \bullet m\mathbf{c} + C$$

$$\ln f = A \tfrac{1}{2} mc'^2 + A \tfrac{1}{2} mc_0^2 + \cancel{m\left(A\mathbf{c}_0 + \mathbf{B}\right) \bullet \mathbf{c}'} + \cancel{\mathbf{B} \bullet m\mathbf{c}_0} + C$$

$A \tfrac{1}{2} m = -\beta$ negative since the distribution is bounded

$$f = \exp\left(C + \beta^2 c_0^2\right) \exp\left(-\beta^2 c'^2\right)$$

$$\exp\left(C + \beta^2 c_0^2\right) = \beta^3 \big/ \pi^{3/2}; \qquad \beta^2 = \frac{m}{2kT}$$

Thermal Speeds

$$c_p = \sqrt{\frac{2kT}{m}}$$ The most probable molecular thermal speed

$$c_{av} = \frac{2}{\sqrt{\pi}} c_p$$ The average thermal speed

$$c_{ms} = \frac{3kT}{m}$$ The mean square thermal speed

$$c_s = \sqrt{\frac{3\pi}{8}} c_{av}$$ The root mean thermal speed

$$a_s = \sqrt{\gamma \frac{kT}{m}}$$ The speed of sound

THE JOURNAL OF CHEMICAL PHYSICS VOLUME 56, NUMBER 5 1 MARCH 1972

Low-Energy Repulsive Interaction Potential for Helium

P. Cantini, M. G. Dondi, G. Scoles, and F. Torello

Gruppo Nazionale di Struttura della Materia del C.N.R., Istituto di Scienze Fisiche dell'Università, Genova, Italy

(Received 21 December 1970)

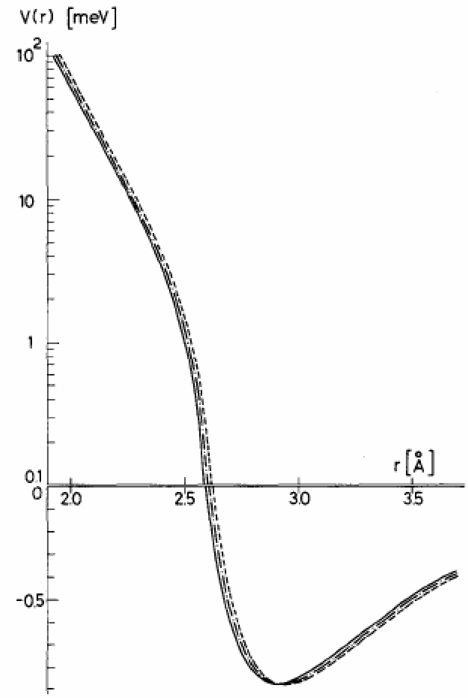

Fig. 11. All potentials are L-J (12, 6) with $\epsilon = 0.874$ meV, (—) $r_m = 2.91$ Å; (-·-) $r_m = 2.93$ Å; (- - -) $r_m = 2.95$ Å.

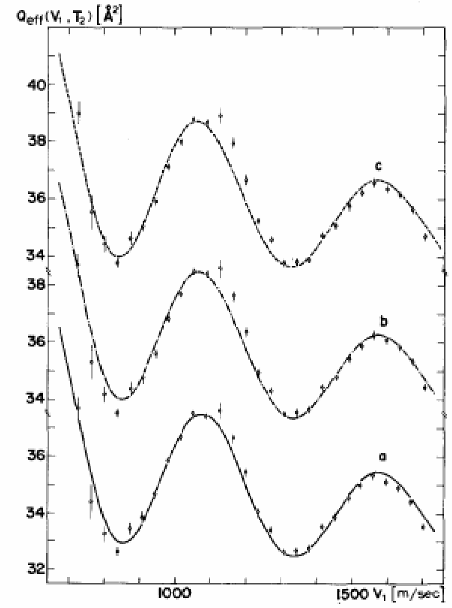

Fig. 12. Comparison between $Q_{expt1}(v_1)$ and $Q_{eff}(v_1)$ computed using: (a) potential No. 5 of Table II; (b) potential 16 (MDD-1); (c) potential 18 (MDD-2).

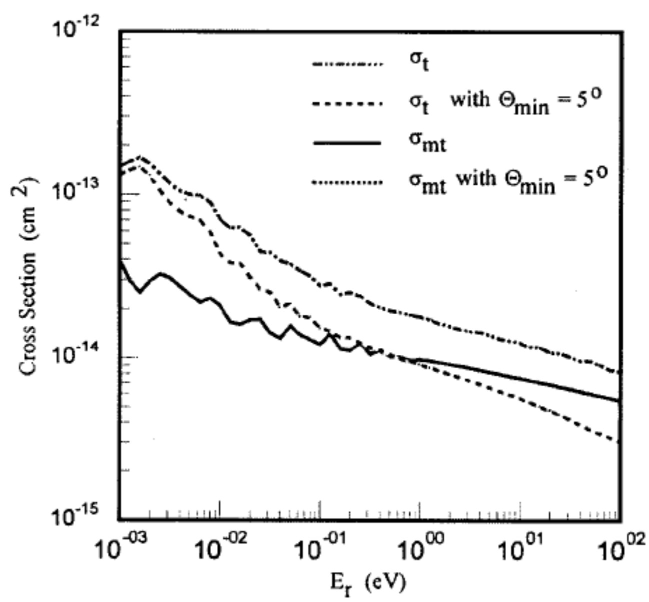

FIG. 1. Comparison of total and momentum transfer cross sections for $D^+ + D$ collisions with and without the small-angle cut-off approximation.

Phys. Plasmas, Vol. 7, No. 12, December 2000

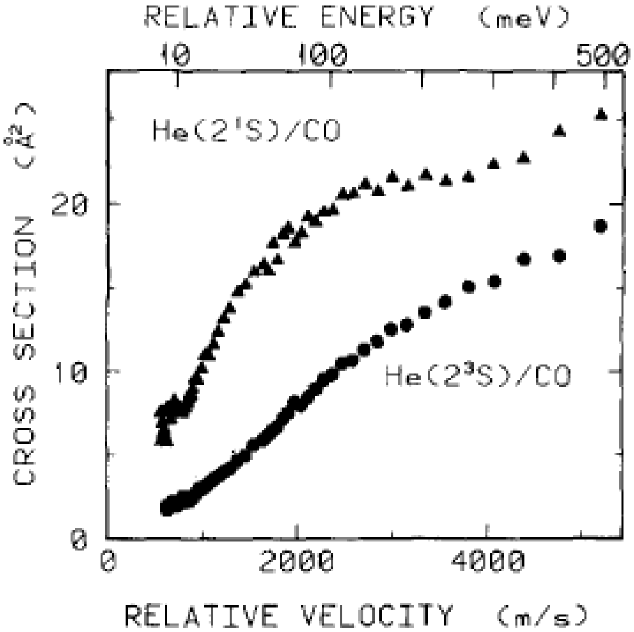

FIG. 11. Total ionization cross sections for CO: ▲, singlet; ●, triplet.

J. Chem. Phys., Vol. 76, No. 1, 1 January 1982

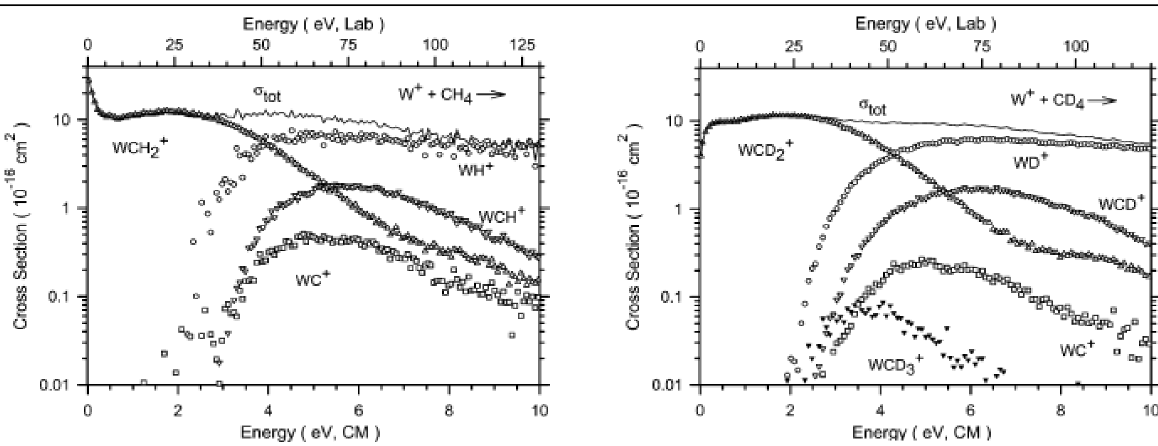

Figure 1. Cross sections for reactions of W^+ with CH_4 (at 0.15 mTorr, part a) and with CD_4 (at 0.28 mTorr, part b) as a function of kinetic energy in the center-of-mass (lower axis) and laboratory (upper axis) frames.

$$W^+ + CH_4\,(CD_4) \rightarrow WCH_3^+\,(WCD_3^+) + H\,(D)$$

$$\rightarrow [W,C,2H]^+\,([W,C,2D]^+) + H_2\,(D_2)$$

$$\rightarrow WCH^+\,(WCD^+) + H_2\,(D_2) + H\,(D)$$

$$\rightarrow WC^+ + 2\,H_2\,(D_2)$$

$$\rightarrow WH^+\,(WD^+) + CH_3\,(CD_3)$$

PE Surface for Methane Activation by W^+

J. Phys. Chem. A, Vol. 110, No. 4, 2006

Ion Mobility Time-of-Flight Mass Spectrometry

$$K = \frac{v_d}{E},\ \{cm^2 V^{-1} s^{-1}\}$$

$$K = \frac{L^2}{Vt_d} = \frac{L}{Et_d}$$

electric field vs. potential

$$K_0 = K\left(\frac{273.15K}{T(K)}\right)\left(\frac{P(Torr)}{760Torr}\right)$$

$$K = \left(\frac{3q}{16N}\right)\left(\frac{2\pi}{\mu kT}\right)^{\frac{1}{2}}\left(\frac{1}{\sigma_M}\right),\ eq.Chapmen - Enskog$$

$$\sigma_M = \int_0^{4\pi} \sigma(1-\cos\chi)\,d\Omega = 2\pi\int_0^{\pi} \sigma(1-\cos\chi)\sin\chi\,d\chi$$

The momentum transfer (diffusion) cross-section

Relation between mobility and diffusion

has long been expected on physical grounds, and it is now well understood how to produce such a relation on the basis of solutions of the Boltzmann equation:

$$\frac{qD}{K} = kT,\ eq.\text{Nernst-Townsend-Einstein}$$

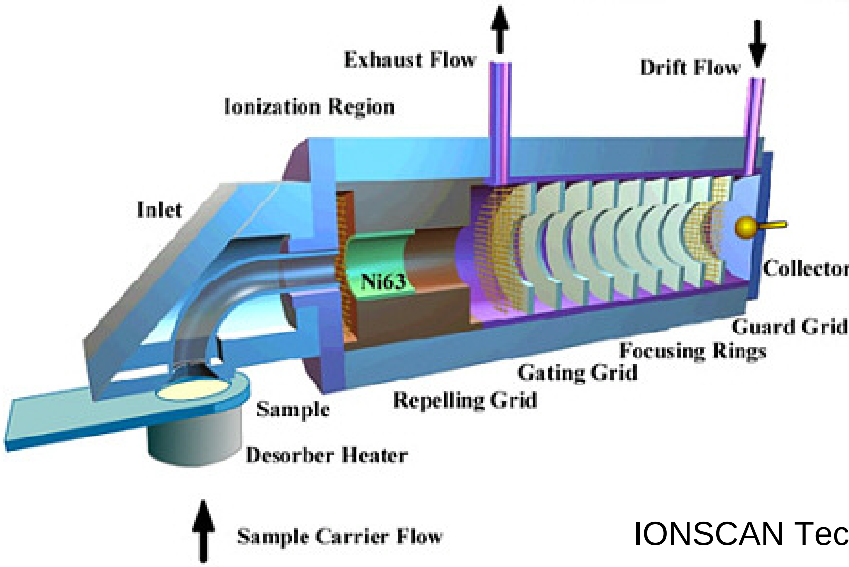

IONSCAN Technology

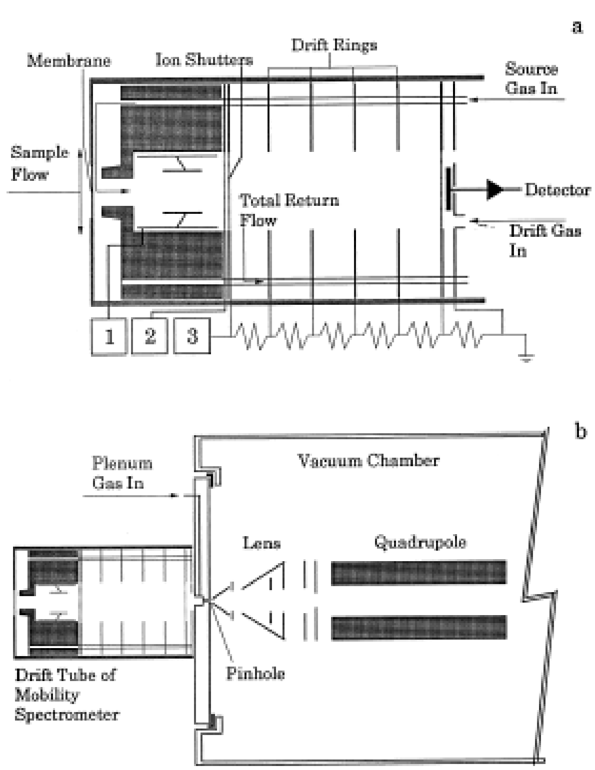

Fig. 1. Schematic diagram of (a) the ion mobility spectrometer and (b) the mobility spectrometer-mass spectrometer. Labels 1, 2, and 3 are, respectively, the high voltage supplies for the ion source, the shutter, and the drift tube.

R.G. Ewing et al./International Journal of Mass Spectrometry 193 (1999) 57–68

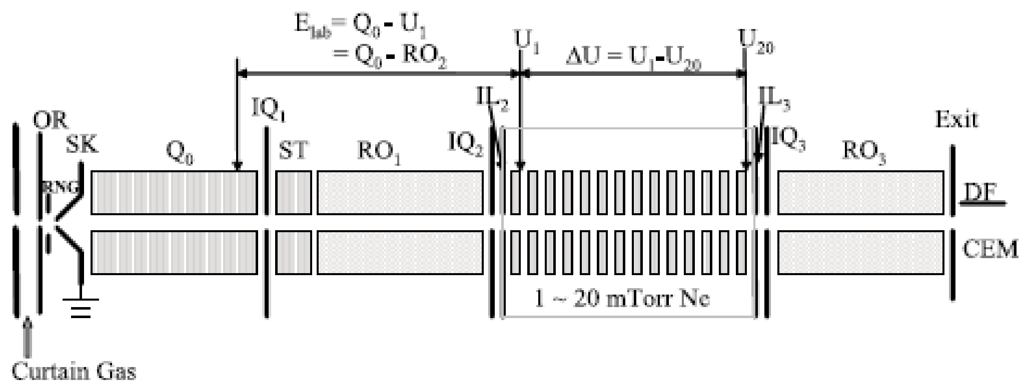

Figure 1. Schematics representation of the experimental setup: Q_0: RF-only ion guide (-7V normally); RO_1 and RO_3: DC offset of quadrupole mass analyzers (normally RO_1=-8.4 V, RO_3=U_{20} -5V for MS/MS scan); IQ_1, IQ_2 and IQ_3: electrostatic lenses (IQ_1 = -7.5V, IQ_2 = -27V and IQ_3 = U_{20} -5V); IL_2, IL_3: additional HP-SQCC enclosure lenses (IL_2 = -7V; IL_3 = U_{20}-5V); ST: short RF-only prefilter (-7V); E_{lab}: ion energy defined in lab frame; RO_2: DC offset of HP-SQCC (-7V); ΔU: DC potential between the first and last segments equally distributed along 20 segments; U_1, U_{20}: DC offset of the first and last segment (U_1 = RO_2 = -7V;U_{20} = U_1-ΔU).